Int J Adv Manuf Technol (2016) 86:2291–2300
DOI 10.1007/s00170-016-8357-2

ORIGINAL ARTICLE

Three-dimensional stability prediction and chatter analysis in milling of thin-walled plate

Sheng Qu[1,2] · Jibin Zhao[1] · Tianran Wang[1]

Received: 20 November 2015 / Accepted: 13 January 2016 / Published online: 25 January 2016

Abstract Stability lobe diagram can be used for selecting proper milling parameters to perform chatter-free operations and improve productivity during milling of thin-walled plates. This paper studies the machining stability in milling of thin-walled plates and develops a three-dimensional stability lobe diagram of the spindle speed, tool position, and axial depth of cut. The workpiece-holder system is modeled as a 2-degree-of-freedom system considering that the tool system is much more rigid than the thin-walled plate, and dynamic equations of motion described for the workpiece-holder system are solved numerically in time domain to compute the dynamic displacements of the thin-walled plate. Statistical variances of the dynamic displacements are then employed as a chatter detection criterion to acquire the stability lobe diagram. The experimentally obtained stability limits correspond well with the predicted stability limits. In addition, influence of feed rate on stability limits is also investigated. By performing frequency analysis of the measured cutting forces to judge if chatter occurs, it is found that feed per tooth has little influence on the stability limits. However, feed per tooth impacts the machined surface quality. The results show that the surface quality drops by increasing feed per tooth.

✉ Sheng Qu
qusheng@sia.cn

Jibin Zhao
jbzhao@sia.cn

[1] Shenyang Institute of Automation, Chinese Academy of Sciences, Shenyang 110016, China

[2] University of Chinese Academy of Sciences, Beijing, China

Keywords Three-dimensional stability lobe · Chatter · Feed per tooth · Thin-walled plate

1 Introduction

Chatter has a negative influence on machining quality and productivity even for high-speed milling due to the regenerative effect. It also causes cutting tool damage and excessive noise. Conservative milling conditions are often adopted to ensure stable milling, which limits the advantage of high performance machining. These effects have encouraged scholars to develop different theories and models for predicting and avoiding this phenomenon. The recent industrial demands for more and more thin-walled plates, which have large area and low rigidity. This has stimulated the development of chatter model in end milling of thin-walled plates for the purpose of high productivity and quality.

Scholars in this field usually focus on dynamic model of the tool-holder-spindle assembly and the construction of stability lobe diagram. Several studies have been put forward to get the stability boundary analytically or semi-analytically in the past two decades. Altintas and Budak [1] proposed the first analytically approach using the zeroth order approximation to predict stability lobes directly in the frequency domain. Merdol and Altintas [2] put forward the multifrequency solution for low radial immersion milling. Davies et al. [3] utilized the time-domain solution technique for predicting the stability of highly interrupted machining. Mann et al. [4] took advantage of the temporal finite element analysis (TFEA) method in order to approximate the milling process more accurately, which made it possible for obtaining the surface location error and stability simultaneously. Insperger and Stepan [5] proposed the semi-discretization method (SDM), which discretized the delay

term only and transformed the original delay differential equations (DDE) into a series of ordinary differential equations with known solutions. This method improves the stability simulation accuracy of low immersion and is widely used for predicting stability of various milling operations. Ding et al. proposed the full-discretization method (FDM) [6] and numerical integration method (NIM) [7] based on the direct integration scheme. Besides, these methods do not lose any numerical precision and have higher computational efficiency than the SDM. Li et al. [8] introduced a complete discretization scheme for milling stability analysis. In this method, all time-dependent items of the DDE were discretized. Compean et al. [9] proposed an enhanced multistage homotopy perturbation method to obtain the stability. Recently, Ding et al. [10] and Huang et al. [11] proposed efficient yet simple semi-analytical time-domain methods to analyze stability. But the method in ref. [11] is based on linear acceleration approximation. The aforementioned stability lobe diagrams are two-dimensional. Several researchers also devoted to three-dimensional stability lobe diagram and achieved some developments. Thevenot et al. [12] developed a three-dimensional stability lobe diagram of the spindle speed, axial depth, and tool position with a constant radial depth, taking the dynamic behavior variation of the part with respect to the cutter position into account. Tang [13] adopted the zero-order solution and constructed the lobe diagram in milling the thin-walled plate incorporating spindle speed, radial, and axial depth of cut. In addition, Quintana et al. [14] identified the stability lobe diagram using the experimental method.

Researches on chatter detection have been developed by monitoring certain signals from different types of sensors in the past years, such as cutting forces [15], vibration [16], and sound [17]. The acquired signals are analyzed by different methods so as to find chatter features. Chatter vibration is identified by implementing intelligent recognition or setting apt thresholds of chatter features. Quintana and Ciurana [18] recognized chatter based on efficient signal processing algorithms. Mann et al. [19] proposed an acceptable detection method by Fourier transform analysis. Khalifa et al. [20] tried to apply image-process techniques to recognize the presence of chatter. Tangjitsitcharoen [21] identified chatter by spectrum analysis based on the power spectrum density. Wang and Liang [22] analyzed discrete wavelet transform statistically to detect chatter. Cao et al. [23] presented an efficient method in end milling based on Hilbert-Huang transform. Li et al. [24] and Afazov et al. [25] employed statistical variances as a chatter detection criterion in time domain. Chatter detection aims at chatter suppression. Various effective strategies have been utilized to suppress chatter, such as vibration absorbers [26] and tuned viscoelastic dampers [27]. Tsai et al. [28] investigated spindle speed regulation and acoustic signal feedback to prevent chatter. Abele et al. [29] implemented piezoelectric active vibration control systems for chatter avoidance. Huang et al. [30] proposed to disrupt chatter by a variable pitch cutter.

A great deal of research has been conducted in the conventional machining chatter model in the past years. But there are still knowledge gaps in the chatter model of milling thin-walled plate. The 2D stability lobe diagram sometimes is not comprehensive to describe the stability of the chatter system. This paper is based on a chatter model in time domain to determine the three-dimensional stability lobe diagram when milling the thin-walled plate. The 3D stability lobe diagram is obtained by the combination of chatter detection and analytical algorithm. That is, the modal parameters at different tool positions are measured and then applied to the chatter model. Statistical variances of the thin-walled plate displacements are adopted as a chatter detection criterion in time domain. According to the developed 3D stability lobes, we can select appropriate parameters to avoid chatter and improve the machining efficiency all through the machining process. Influence of feed per tooth on stability lobes is also investigated, which contributes to increasing material removal rate.

2 Chatter model in time domain

The workpiece is assumed to be thin and cantilevered, shown in Fig. 1. It is clamped at one end, free in the X and Y directions. The flat end milling cutter is treated as a rigid body while the workpiece-holder system is considered flexible. Provided that the whole tool system is more rigid than the thin-walled plate, attention should be paid to the dynamics of the workpiece-holder system. The workpiece-holder system can be reduced to a 2-degree-of-freedom as shown in Fig. 2, where the rigidity in the Z direction is supposed to be high when compared to the other two directions. X

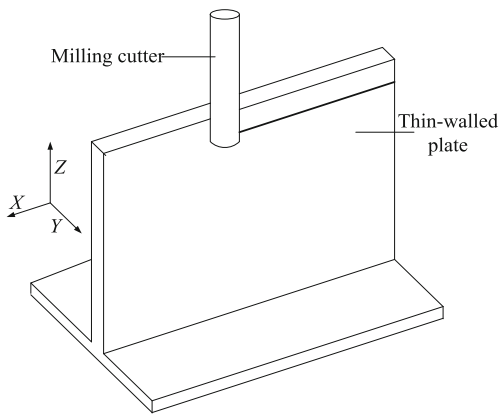

Fig. 1 Thin-walled plate in end milling

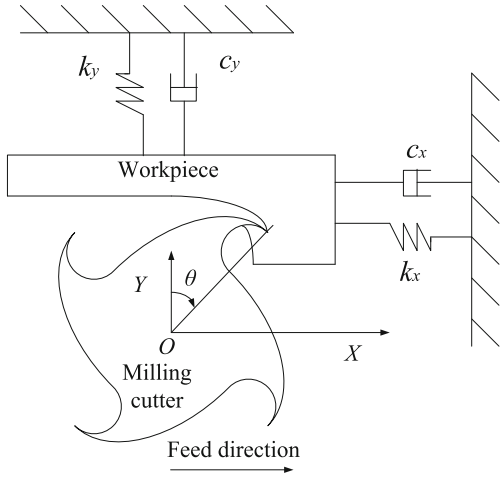

Fig. 2 Dynamic model of the system

and Y are the directions of feed and perpendicular to the machined surface, respectively. When machining the thin-walled plate, chatter usually occurs on the surface normal to the direction of cutting velocity.

$m_a, c_a, k_a (a = x, y)$ represent the modal mass, modal damping, and modal stiffness of the workpiece-holder system in the two directions, respectively. These modal parameters can be deduced by using impact hammer test where the frequency response function (FRF) is determined. The dynamics of the workpiece-holder system are described by following two second-order ordinary differential equations for each degree-of-freedom [25]:

$$\begin{cases} m_x\ddot{x}(t) + c_x\dot{x}(t) + k_x x(t) = F_x(f, a_p, r, \Delta, \omega, t) \\ m_y\ddot{y}(t) + c_y\dot{y}(t) + k_y y(t) = F_y(f, a_p, r, \Delta, \omega, t) \end{cases} \tag{1}$$

where f is the feed per tooth, a_p is axial depth of cut, r is the radius of the cutter, Δ is the phase angle between two adjacent teeth, ω is the spindle angular velocity, t is the time.

Through infinitesimal treatment of the milling cutter, the tangential force F_t, radial force F_r and axial force F_a on the axis unit are proportional to the instantaneous undeformed chip thickness h and can be expressed as [24]:

$$\begin{cases} F_t = k_{tc} h dz + k_{te} dz \\ F_r = k_{rc} h dz + k_{re} dz \\ F_a = k_{ac} h dz + k_{ae} dz \end{cases} \tag{2}$$

where $k_{tc}, k_{rc}, k_{ac}, k_{te}, k_{re}$, and k_{ae} are collectively referred to as the cutting force coefficients, dz is axis depth of cut. The chip thickness h is calculated based on the work of Qu et al. [31]. Cutting force is divided into shearing force caused by shearing in the shear zone, and ploughing force derived from flank surface friction of the cutting edge. And on the condition that the instantaneous position angle of the tooth tip is θ, the cutting forces can be deduced:

$$\begin{pmatrix} F_x \\ F_y \\ F_z \end{pmatrix} = \begin{pmatrix} -\cos\theta & -\sin\theta & 0 \\ \sin\theta & -\cos\theta & 0 \\ 0 & 0 & 1 \end{pmatrix} \begin{pmatrix} F_t \\ F_r \\ F_a \end{pmatrix} \tag{3}$$

With the help of the software MATLAB, the fourth order of precision Runge-Kutta method is used to solve Eq. 1 in time domain solution by integrating the differential equations. Then, the dynamic displacements of the workpiece in the X and Y directions can be figured out. Statistical variances the dynamic displacements are employed as a criterion to detect chatter. The statistical variances can be given by [32]

$$\sigma_x^2 = \frac{\sum_{i=1}^{n}(x_i - \overline{x})^2}{n-1}; \sigma_y^2 = \frac{\sum_{i=1}^{n}(y_i - \overline{y})^2}{n-1} \tag{4}$$

where ${\sigma_x}^2$ and ${\sigma_y}^2$are the statistical variances in the X and Y directions, n is the number of time increments, x_i and y_i are the displacements of the workpiece in the X and Y directions calculated from Eq. 1, $\overline{x}$ and $\overline{y}$ are the average displacements in the two directions. They are depicted as:

$$\overline{x} = \frac{\sum_{i=1}^{n}(x_i)^2}{n-1}; \overline{y} = \frac{\sum_{i=1}^{n}(y_i)^2}{n-1} \tag{5}$$

It is considered that chatter occurs when the statistical variances are bigger than the value of 1 μm^2, for example see Li et al. [24] and Afazov et al. [25]. In other words, if the statistical variance in the X and Y direction reaches 1 μm^2, the system is in the critical state and the minimum stability is determined. The flow chart of the algorithm to determine the stability lobe diagram is shown in Fig. 3.

3 Three-dimensional stability lobe

3.1 Test of modal parameters

The modal parameters of the milling system should be tested before predicting the stability. Impact hammer test is the most common approach to measure these dynamic parameters. The dynamic signal analysis system CRAS is used to measure FRF in the impact test. Figure 4 shows the experimental setup. A accelerometer attached to the thin-walled plate is used for measuring the corresponding acceleration caused by the exciting force. The collected acceleration signals are analyzed to determine the FRF of the system. Then, the dynamic modal parameters are derived by the peak-picking curve fitting method.

The size of the thin-walled plate in this study is 120 × 100 × 6 mm. The material of the workpiece selected for experiments is die steel NAK80, the hardness of which is HB 344-400. The part is machined on ME650 three-dimensional vertical machining center. The cutter used in

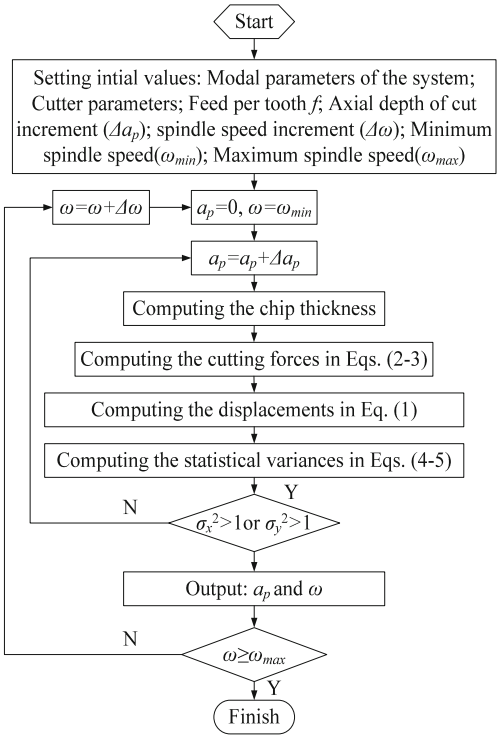

Fig. 3 Flow chart of the algorithm to determine the stability lobe diagram

experiments is a four-flute flat-end milling cutter (diameter 16 mm, nose radius 0.25 mm, and helix angle 30°) with its overhang length 48.3 mm, which is made of solid carbide and coated with TiSiN. According to experimental results, the stiffness of the tool-spindle system is ten times more than that of the thin-walled plate. Hence, dynamic displacements of the wall are applied to calculate statistical variances for verifying whether chatter occurs.

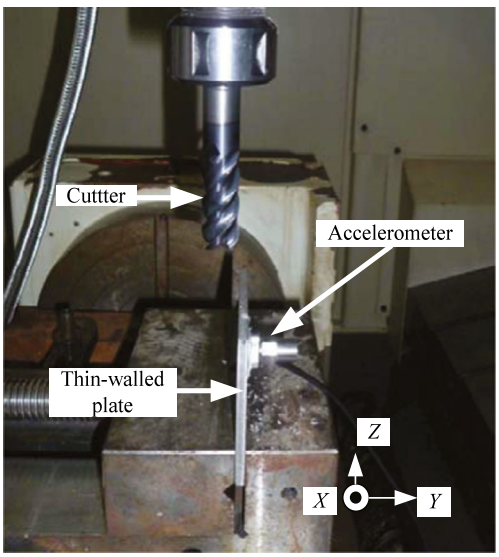

Fig. 4 Experimental setup for thin-walled plate impact test

The dynamic properties of the thin-walled plate depend on the tool position, which is mobile along L (Fig. 5). The stiffness and damping of the wall will be continuously changing as the tool position changes. So the dynamics of the process can be represented, respectively, according to the tool position. Considering the variation in the dynamics of the wall, the wall is divided into several zones at the same height and impact tests are conducted in each zone to obtain corresponding dynamics. It is assumed that the variation of dynamic parameters resulting from material removal is neglected in each zone. Hence, the more zones the wall is divided into, the more accurate the acquired modal parameters are. In this study, the thin-walled plate is divided into four zones, shown in Fig. 5. Points A, B, C, and D are located in the central of each zone, respectively. When the tool reaches these points, the milling process is interrupted and the accelerometer is attached to these points to measure the acceleration signals caused by impact test.

Through the developed method, the modal parameters of the workpiece-holder system in different zones are acquired. Table 1 shows the obtained modal parameters at the top of the wall in the X and Y directions. The radial depth of cut is 1 mm, and the axial depth of cut is 2.7 mm.

3.2 Stability lobes and experiment verification

In order to ensure the accuracy and efficiency of the algorithm to obtain the stability, axial depth of cut increment Δa_p is 0.02 mm and spindle speed increment $\Delta\omega$ is 100 rev/min in this study. In addition, the feed per tooth f is 0.15 mm. Based on the flow chart in Fig. 3, the stability lobe

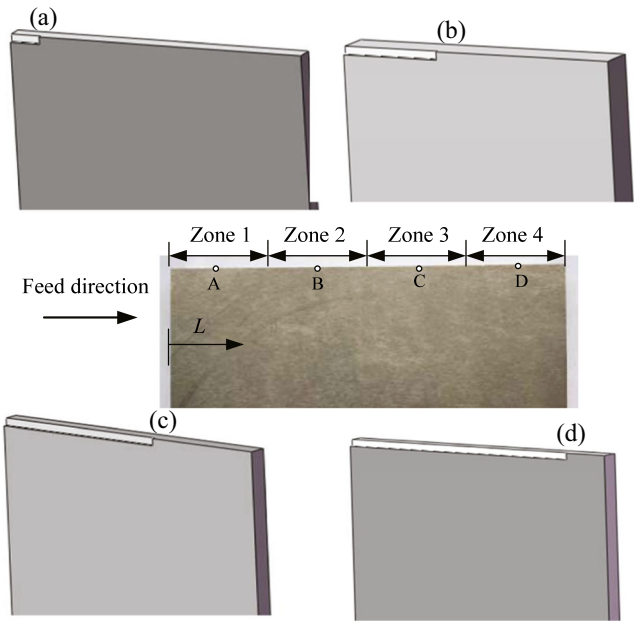

Fig. 5 Divided zones used for measuring modal parameters

Table 1 Modal parameters of the workpiece-holder system at the top of the wall

	In the *X* direction			In the *Y* direction		
	Mass	Damping	Stiffness	Mass	Damping	Stiffness
Zone 1	0.641 kg	305.33 N/(m/s)	1.25*e*7 N/m	0.304 kg	144.81 N/(m/s)	2.56*e*6 N/m
Zone 2	0.639 kg	298.51 N/(m/s)	1.22*e*7 N/m	0.284 kg	132.47 N/(m/s)	2.37*e*6 N/m
Zone 3	0.633 kg	289.49 N/(m/s)	1.24*e*7 N/m	0.311 kg	139.70 N/(m/s)	2.54*e*6 N/m
Zone 4	0.624 kg	283.62 N/(m/s)	1.17*e*7 N/m	0.294 kg	136.69 N/(m/s)	2.42*e*6 N/m

of the spindle speed and axial depth of cut is presented in Fig. 6 by using MATLAB software. The stability is derived in the spindle speed range from 2000 to 16,000 rev/min. And the modal parameters in zone 2 are adopted in the simulation.

The stiffness and damping of the wall will be dropping as more material is removed. The dynamic behavior of the wall depends on the position of the tool. The variation in the dynamics of the wall due to material removal cannot be neglected, which leads us to a three-dimensional lobe diagram construction. Thus, the tool position is introduced in the stability lobe diagram.

The steps to obtain the three-dimensional stability lobe diagram are as follows. First of all, we need to identify the modal parameters in the first tool position and acquire the two-dimensional stability lobe based on the flow chart in Fig. 3. Then, repeat the previous step and plot two-dimensional stability limits in all tool positions. Finally, these acquired two-dimensional stability limits are analyzed by MATLAB and then the three-dimensional stability lobe diagram is determined. Figure 7 shows the three-dimensional stability lobe diagram of the spindle speed, tool position, and axial depth.

The upper side of the curved surface in Fig. 7 is unstable zone, and the down side of that is stable zone. Figure 7 illustrates that the maximum axial depth under the condition of chatter-free gradually decreases with the increment of tool position L when the spindle speed is fixed. So one can select appropriate milling parameters to avoid chatter and improve productivity as well according to the curved surface in Fig. 7.

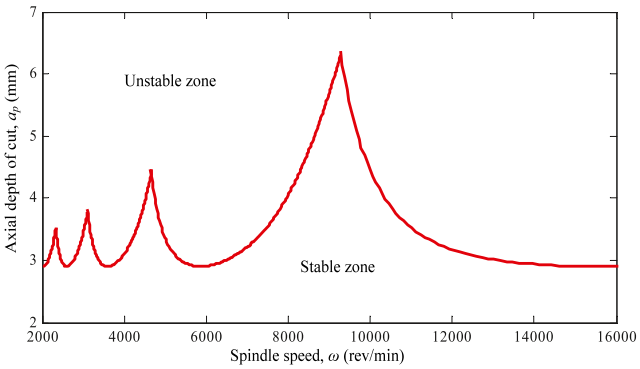

Fig. 6 Stability lobe diagram when feed per tooth f is 0.15 mm

Typically, frequency analysis of cutting forces or acceleration signals is helpful to judge if chatter occurs. It is widely known that peak values of cutting forces or acceleration signals occur at the integral multiples of spindle frequency (SF) in a stable milling process. In contrast, if the peak values appear at some different frequencies from the multiple of SF, the presence of chatter can be surmised.

Nine groups of up milling experiments in zone 2 are performed from 2000 to 10,000 rev/min spindle speed with increment of 1000 rev/min and constant feed per tooth of 0.15 mm. The radial depth of cut a_e is a fixed value 1 mm. All these milling experiments are carried out at the same height, the top of the wall. In each group of milling experiments, the axial depth of cut starts from 2.1 mm and increases 0.2 mm after finishing every experiment. The cutting forces in the X and Y directions are measured by Kistler 9257B and analyzed by the fast Fourier transform (FFT) in the frequency domain. Subsequently, we can assess whether chatter occurs from frequency spectra distributions of the cutting forces. Table 2 shows the initial axial depths of cut when chatter happens and the maximum axial depth of cut without chatter determined experimentally at different spindle speeds when feed per tooth is 0.15 mm and radial depth of cut is 1 mm.

The comparison between the proposed theoretical chatter model and the experimentally acquired stability limits is presented in Fig. 8. It can be seen that the initial axial depths of cut determined experimentally when chatter happens correspond well with the predicted stability lobes. However, at spindle speed of 10,000 rev/min, the experimentally obtained initial axial depth of cut is a little lower than the predicted one.

4 Influence of feed per tooth on stability lobes

The feed rate effect on the stability is investigated based on the proposed chatter model. Several simulations are implemented with the same parameters except the feed per

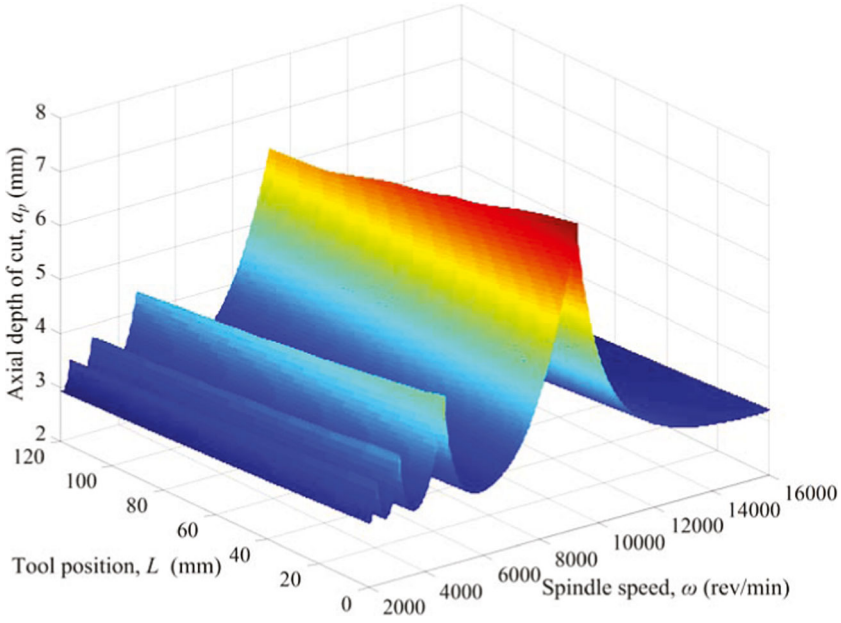

Fig. 7 Three-dimensional stability lobes

tooth f. Figure 9 shows the simulated stability lobes with f = 0.05, 0.10, 0.20, and 0.25 mm. Compared to Fig. 6, these simulated stability limits are almost the same. The stability limits do not change obviously as feed rate increases or decreases.

To verify the influence of feed per tooth on the chatter stability, several milling scenarios are performed. If the feed rate has an influence on the stability, the stability limits will increase or decrease as the change of feed rate. Otherwise, the stability limits remain unchanged even if changes have taken place in feed rate. Hence, according to Table 2, we select the maximum axial depth of cut without chatter as the axial depth of cut to detect whether chatter occurs when feed per tooth is changed in an available range.

Several groups of up milling experiments are carried out from 2000 to 10,000 rev/min spindle speeds with increment of 1000 rev/min. According to Table 2, the axial depth of cut is set as the the maximum axial depth of cut without chatter at a specific spindle speed with fixed radial depth of cut 1 mm. For example, the axial depth of cut is 3.7 mm when spindle speed is 8000 rev/min. And at the specific spindle speed, the feeds per tooth are are set as 0.05, 0.10, 0.20, and 0.25 mm, respectively. The cutting forces in the X and Y directions at different feed rates are measured by dynamometer.

Take the cutting force data in the milling experiments at spindle speed of 8000 rev/min to analyze whether chatter occurs if feed per tooth decreases or increases. Figure 10 shows the measured cutting forces in the Y direction at different feed rates. The maximum cutting force in the Y direction is less than 180 N when f = 0.15 mm (Fig. 10c). By decreasing f to 0.05 mm while other parameters are kept constant, the maximum cutting force decreases to less than 100 N (Fig. 10a). Similarly, by increasing f to 0.25 mm, the maximum cutting force grows to almost 300 N (Fig. 10e). It is observed that cutting force improves as feed per tooth increases. However, the cutting processes are stable despite the fact that feed rate increases or decreases.

Waterfall plots of the FFT harmonics of the cutting forces in the Y direction at different feed rates per tooth are shown in Fig. 11. SF is defined as SF $= \frac{\omega}{60}$. When spindle speed ω is 8000 rev/min, SF is 133.3 Hz. It is observed from Fig. 11 that their frequency spectra distributions are periodic. The peak values at the multiplies of SF are noted, and

Table 2 Axial depths of cut determined experimentally at different spindle speeds

Spindle speed (rev/min)	2000	3000	4000	5000	6000	7000	8000	9000	10,000
Initial axial depth With chatter (mm)	2.7	3.3	3.1	2.9	2.7	2.9	3.9	5.1	3.5
Maximum axial depth Without chatter (mm)	2.5	3.1	2.9	2.7	2.5	2.7	3.7	4.9	3.3

a_e = 1 mm, f = 0.15 mm

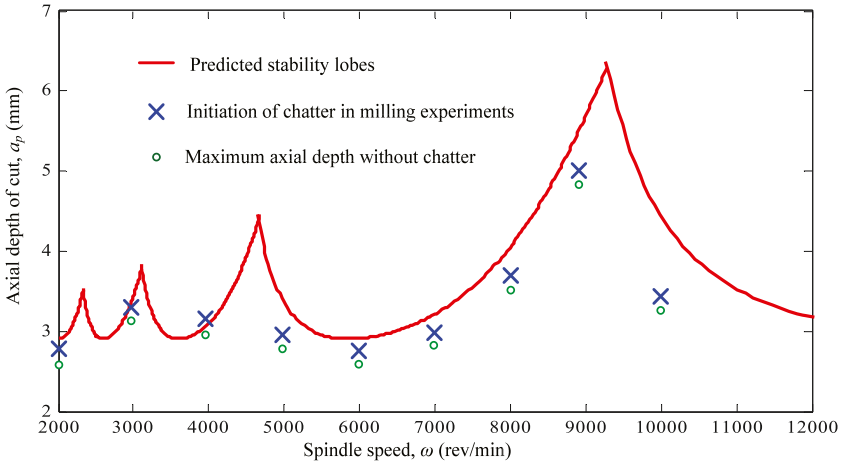

Fig. 8 Stability lobes determined theoretically and experimentally

the FFT harmonics at other frequencies are almost none. In Fig. 11a–c, when feeds per tooth are 0.05, 0.10, and 0.15 mm, the dominant peak values occur at 266.7 Hz (2 × SF) and 533.2 Hz (4 × SF); but when feed per tooth grows to 0.25 mm, the dominant frequency component is 133.3 Hz (Fig. 11e). There is not a significant amplitude occurring at other frequencies in the frequency spectra, which can be deduced that chatter does not occur as feed rate increases or decreases.

The aforementioned experiment results by increasing or decreasing feed rate at 8000 rev/min are also discovered at other spindle speeds. The maximum axial depth without chatter is a fixed value at the specific feed rate and spindle speed. And its value remains unchanged by increasing or decreasing the feed rate while other parameters are kept constant. Namely, the stability limits obtained experimentally do not change along with feed rate. The same results are also found at other tool positions. So it is deduced that feed rate has little influence on the three-dimensional stability lobe diagram, although higher feed per tooth results in higher cutting force.

Maximizing material removal rate is a primary goal in the machine shop environment. Possible methods to increase material removal rate include increasing the spindle speed, axial depth of cut, and feed rate. For the purpose of improving milling efficiency, we select appropriate spindle speeds and axial depths of cut to machine different positions of the thin-walled part according to the three-dimensional stability lobe diagram. We have investigated that feed per tooth has little influence on the three-dimensional stability limits.

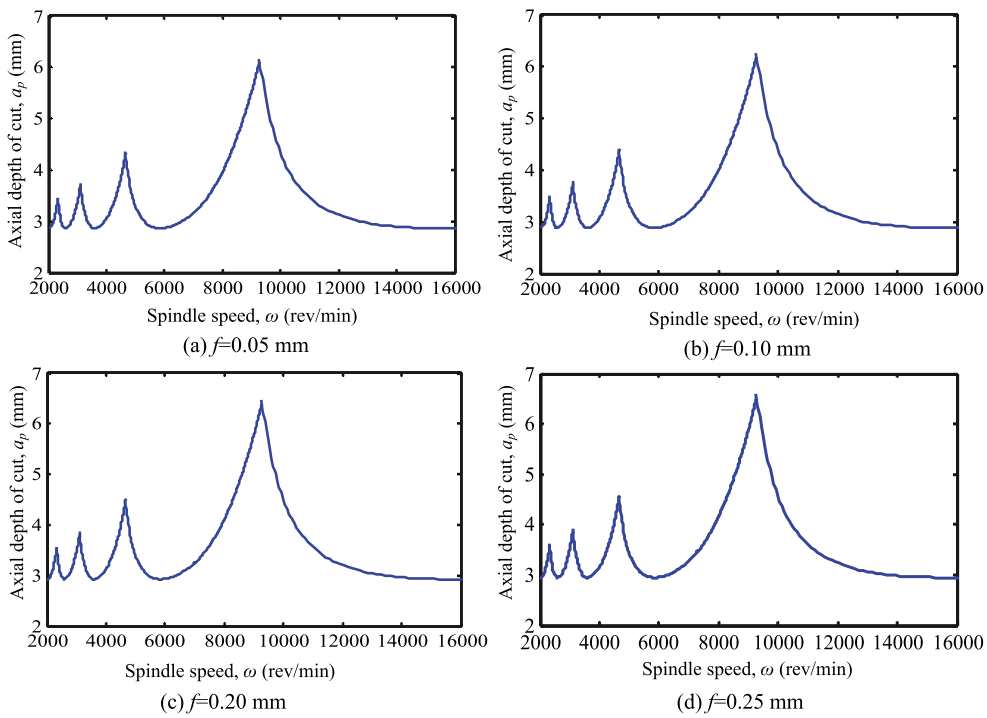

Fig. 9 Stability lobes obtained theoretically at different feed rates

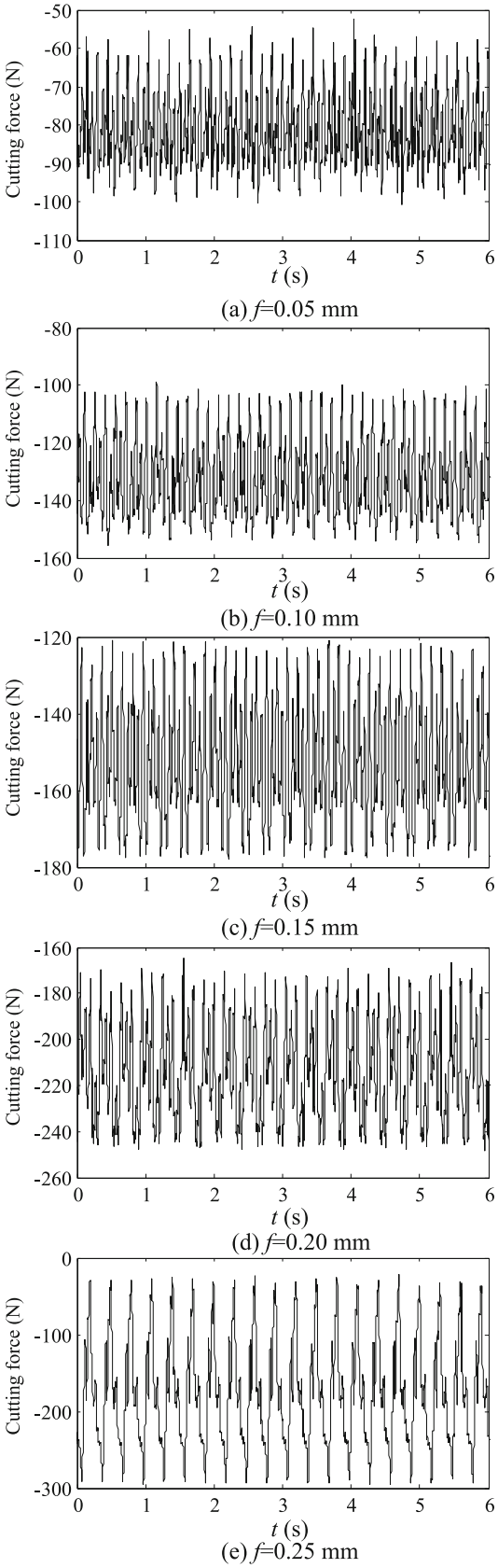

Fig. 10 Cutting forces of Y direction at different feed rates. Up milling, ω = 8000 rev/min, a_e = 1 mm

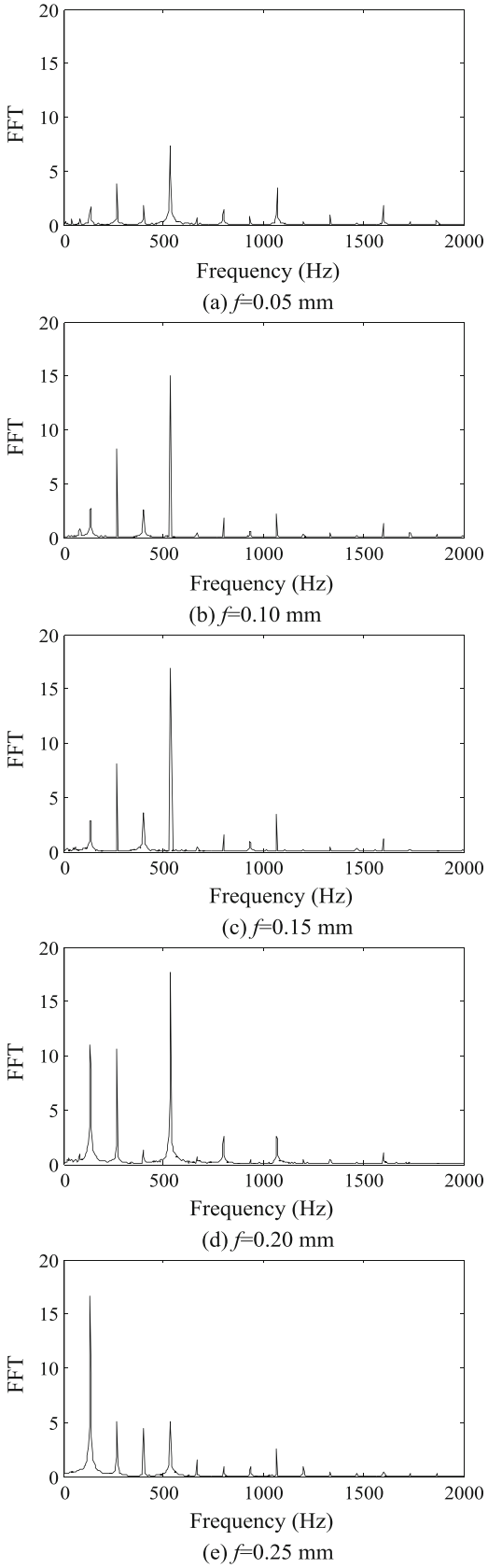

Fig. 11 FFT analysis on the cutting forces in the Y direction at different feed rates

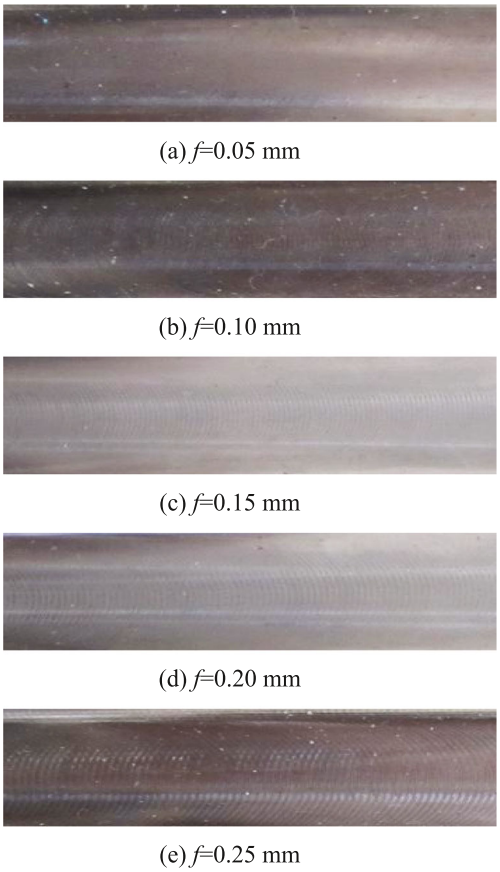

Fig. 12 Machined workpiece surfaces at different feed rates. Milling condition: ω = 8000 rev/min, a_e = 1 mm, up milling

Therefore, when the spindle speed and axial depth of cut are fixed, further increasing productivity can be achieved by increasing feed per tooth at the condition of ensuring the machining quality and chatter-free operations.

Figure 12 gives the machined surfaces at different feeds per tooth and the same spindle speed of 8000 rev/min. The surface roughness curve measured at different feed rated is shown in Fig. 13. It is observed that the increasing feed per tooth causes the rise of the surface roughness value R_a. The reason leading to this trend is because the intensified vibration generated by the increasing cutting force reduces the machined surface quality.

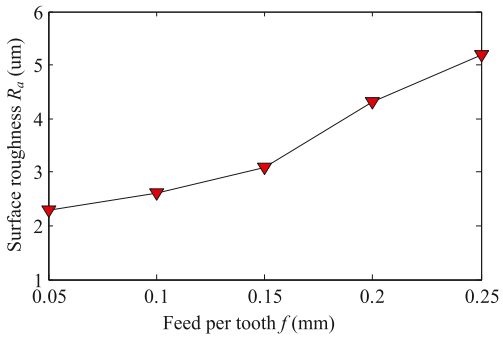

Fig. 13 Surface roughness versus feed per tooth

5 Conclusions

1. A three-dimensional stability lobe diagram based on a chatter model in milling of thin-walled plates is developed in this paper, which can assist in the selection of optimal milling parameters to avoid chatter and improve productivity as well. A third dimension, the tool position, has been introduced in the stability lobe diagram.
2. To verify the predicted stability lobe diagram, nine groups of milling experiments are developed to identify the initial axial depth of cut when chatter occurs at different speeds. The result shows that experimentally obtained stability limits correspond well with the predicted stability limits.
3. The effect of feed rate on stability lobes is investigated. It is observed that feed rate has little influence on the stability lobes within the allowable range of feed rate. Consequently, increasing material removal rate can be further achieved by increasing feed per tooth while the milling is still stable.
4. The surface quality of the machined thin-walled plates drops as feed per tooth increases. This trend is because higher feed rate results in higher cutting force, which intensifies the vibration.

Acknowledgments The authors acknowledge the support from the National Basic Research Program of China (Grant No. 2011CB302400) and the National Natural Science Foundation of China (Grant No. 51175495).

References

1. Altintas Y, Budak E (1995) Analytical prediction of stability lobes in milling. CIRP Ann Manuf Technol 44:357–362
2. Merdol SD, Altintas Y (2004) Multi frequency solution of chatter stability for low immersion milling. J Manuf Sci Eng 126:459–499
3. Davies MA, Pratt JR, Dutterer B, Burns TJ (2002) Stability prediction for low radial immersion milling. J Manuf Sci Eng 124:217–225
4. Mann BP, Young KA, Schmitz TL, Dilley DN (2005) Simultaneous Stability and Surface Location Error Predictions in Milling. ASME J Manuf Sci Eng 127(3):446–453
5. Insperger T, Stepan G (2002) Semi-discretization method for delayed systems. Int J Numer Methods Eng 55(5):503–518
6. Ding Y, Zhu LM, Zhang XJ, Ding H (2010) A full-discretization method for prediction of milling stability. Int J Mach Tools Manuf 50:502–509
7. Ding Y, Zhu LM, Zhang XJ, Ding H (2011) Numerical integration method for prediction of milling stability. J Manuf Sci Eng 133:031005

8. Li M, Zhang G, Huang Y (2012) Complete discretization scheme for milling stability prediction. Nonlinear Dyn 71(1-2):187–199
9. Compean F, Olvera D, Campa F, Lopez de Lacalle L, Elias-Zuniga A, Rodriguez C (2012) Characterization and stability analysis of a multi-variable milling tool by the enhanced multistage homotopy perturbation method. Int J Mach Tools Manuf 57:27–33
10. Ding Y, Zhu LM, Zhang XJ, Ding H (2013) Stability analysis of milling via the differential quadrature method. J Manuf Sci Eng 135:044502
11. Huang T, Zhang XM, Zhang XJ, Ding H (2013) An efficient linear approximation of acceleration method for milling stability prediction. Int J Mach Tools Manuf 74:56–64
12. Vincent T, Lionel A, Gilles D, Gilles C (2006) Integration of dynamic behaviour variations in the stability lobes met hod. Int J Adv Manuf Technol 27:638–644
13. Tang A, Liu Z (2009) Three-dimensional stability lobe and maximum material removal rate in end milling of thin-walled plate. Int J Adv Manuf Technol 43:33–39
14. Quintana G, Ciurana J, Teixidor D (2008) A new experimental methodology for identification of stability lobes diagram in milling operations. Int J Mach Tools Manuf 48:1637–1645
15. Toh CK (2004) Vibration analysis in high speed rough and finish milling hardened steel. J Sound Vib 278(1–2):101–115
16. Kuljanic E, Sortino M, Totis G (2008) Multisensor approaches for chatter detection in milling. J Sound Vib 312(4–5):672–693
17. Schmitz TL (2003) Chatter recognition by a statistical evaluation of the synchro-nously sampled audio signal. J Sound Vib 262(3):721–730
18. Quintana G, Ciurana J (2011) Chatter in machining processes: a review. Int J Mach Tools Manuf 51(5):363–376
19. Mann BP, Insperger T, Bayly PV, Stepan G (2003) Stability of up-milling and down-milling, Part 2: experimental verification. Int J Mach Tools Manuf 43(1):35–40
20. Khalifa OO, Densibali A, Faris W (2006) Image processing for chatter identification in machining processes. Int J Adv Manuf Technol 31:443–449
21. Tangjitsitcharoen S (2009) In-process monitoring and detection of chip formation and chatter for CNC turning. J Mater Proc Technol 209(10):4682–4688
22. Wang L, Liang M (2009) Chatter detection based on probability distribution of wavelet modulus maxima. Robot Comput Integr Manuf 25(6):989–998
23. Cao HR, Lei YG, He ZJ (2013) Chatter identification in end milling process using wavelet packets and Hilbert-Huang transform. Int J Mach Tools Manuf 69:11–19
24. Li ZQ, Liu Q (2008) Solution and analysis of chatter stability for end milling in the time-domain. Chin J Aeronaut 21:169–178
25. Afazov SM, Ratchev SM, Segal J, Popov AA (2012) Chatter modelling in micro-milling by considering process nonlinearities. Int J Mach Tools Manuf 56:28–38
26. Moradi H, Bakhtiari Nejad F, Movahhedy MR (2008) Tunable vibration absorber design to suppress vibrations: an application in boring manufacturing process. J Sound Vib 318:93–108
27. Rashid A, Nicolescu CM (2008) Design and implementation of tuned viscoelastic dampers for vibration control in milling. Int J Mach Tools Manuf 48:1036-1053
28. Tsai NC, Chen DC, Lee RM (2010) Chatter prevention for milling process by acoustic signal feedback. Int J Adv Manuf Technol 47:1013–1021
29. Abele E, Hanselka H, Haase F, Schlote D, Schiffler A (2008) Development and design of an active work piece holder driven by piezo actuators. Production Engineering Research Development 2:437–442
30. Huang PL, Li JF, Sun J, Ge MJ, 2012 Milling force vibration analysis in high-speed-milling titanium alloy using variable pitch angle mill. Int J Adv Manuf Technol 58:153–160
31. Qu S, Zhao JB, Wang TR, Tian FJ (2015) Improved method to predict cutting force in end milling considering cutting process dynamics. Int J Adv Manuf Technol 78:1501–1510
32. Miller I, Freund J (1985) Probability and Statistics for Engineers. Prentice Hall, Englewood Cliffs